

1 Latent Gaussian models to decide on spatial closures
2 for bycatch management in the Barents Sea shrimp
3 fishery

4 Olav Nikolai Breivik^{1*}, Geir Storvik² and Kjell Nedreaas³

5 ¹Department of Mathematics, University of Oslo, P.O. Box 1053 Blindern,
6 0316 Oslo, Norway, Email: olavnb@math.uio.no

7 ²Department of Mathematics, University of Oslo, P.O. Box 1053 Blindern,
8 0316 Oslo, Norway, Email: geirs@math.uio.no

9 ³Institute of Marine Research, P.O. Box 1870 Nordnes, 5817 Bergen,
10 Norway, Email: kjell.nedreaas@imr.no

11 * Corresponding author. Email: olavnb@math.uio.no, Phone: 004793868726, Postal address:
12 Department of Mathematics, University of Oslo, P.O. Box 1053 Blindern, 0316 Oslo, Norway

13 January 4, 2016

15 In the Barents Sea and adjacent water, fishing grounds are closed for shrimp
16 fishing by the Norwegian Directorate of Fisheries Monitoring and Surveillance Ser-
17 vice (MSS) if the expected number of juvenile fish caught are predicted to exceed
18 a certain limit per kilogram shrimp (*Pandalus borealis*). Today, a simple ratio es-
19 timator, which do not fully utilize all data available, is in use. In this research we
20 construct a Bayesian hierarchical spatio-temporal model for improved prediction of
21 the bycatch ratio in the Barents Sea shrimp fishery. More predictable bycatch will
22 be an advantage for the MSS due to more correct decisions and better resource al-
23 location, and for the fishermen due to more predictable fishing grounds. The model
24 assumes that the occurrence of shrimp and juvenile cod can be modeled by linked
25 regression models containing several covariates (including 0-group abundance esti-
26 mates) and random effects modeled as Gaussian fields. Integrated Nested Laplace
27 Approximations (INLA) is applied for fast calculation. The method is applied to
28 prediction of the bycatch ratio for Atlantic cod (*Gadus morhua*).

29 Introduction

30 Trawling for shrimps in the Barents Sea takes place at the seabed, mostly at around
31 200-400 meters depths where the shrimp concentration is highest (Jakobsen and Ozhigin,
32 2011, page 172). To limit the bycatch, and thereby ensure a sustainable ecosystem and
33 fishery in the Barents Sea, rules are made on the amount of bycatch that is allowed.
34 To reduce bycatch, sorting grids were imposed in 1992/1993 (ICES, 1994). A sorting
35 grid is a device on the trawl that sorts out the fish bigger than shrimps and thereby
36 reduces the bycatch. In 1983, the Joint Soviet-Norway Fisheries Commission imposed
37 a regulation that implies that fishing grounds are closed if the expected number of fish
38 caught exceeds a certain limit per kilogram shrimp (Veim et al., 1994). Today this
39 ratio limit is 0.8 for cod, and there are similar rules for bycatch of haddock, redfish
40 and Greenland halibut (Fiskeridirektoratet, 2005). These ratio limits are determined by

41 the biological status of the fish and shrimp stocks, as well as the economical value of
42 the particular fish species (Veim et al., 1994). In this work we investigated bycatch of
43 juvenile cod, but the methodology introduced is general and can be applied to bycatch
44 of other species.

45 The method used today for regulating the shrimp fishery is as follows: When MSS sus-
46 pects that there is a high rate of bycatch in a certain area, an inspector from MSS joins
47 or rents a trawler and counts the number of juvenile cod caught as bycatch by new trawl
48 hauls in that area. The bycatch ratio is then predicted by dividing the total number of
49 juvenile cod by the total catch of shrimps. Based on this prediction a decision is made
50 whether to close the area. After an area is held closed for some time (often some months),
51 data from new trawl hauls are collected and a decision whether to open is made.

52 A statistical modeling approach for prediction of the bycatch ratio of cod in the Barents
53 Sea shrimp fishery has previously been presented in Aldrin et al. (2012). The model
54 considered in this paper is an extension of their model. The main extension from a
55 statistical point of view is that all the parameters in our model are modeled simultaneously
56 and that a Bayesian approach is applied. This results in a more statistical rigorous method
57 to estimate the parameters and to quantify the uncertainty. We use integrated nested
58 Laplace approximations (INLA, Rue et al., 2009, Martins et al., 2013) for performing the
59 calculations involved. The INLA-technique is implemented in the user-friendly R-INLA
60 package in R (R Core Team, 2014, the R-INLA package can be downloaded from <http://www.r-inla.org>). R-INLA has recently been used to model bycatch of Greenland
61 sharks in the Greenland halibut fishery (Cosandey-Godin et al., 2014). Our paper goes
62 further in constructing methodology for decisions as well as also providing models for
63 catch of targeted species.
64

65 The main extension from a biological point of view is that we included several important
66 explanatory variables. New variables considered are, among others, abundance estimates
67 of 0-group cod (juvenile cod less than one year old) in the Barents Sea, the distance
68 trawled and the type of trawling equipment used. In particular, a connection between

69 the yearly strength of the 0-group of cod in the Barents Sea and the bycatch of juvenile
70 cod is of biological interest. Before September/October, the 0-group lives in the upper
71 layers of the sea and grows to around the same size as the shrimps (mean length about
72 8 cm Ottersen and Loeng, 2000). After September/October the 0-group changes to a
73 demersal life stage, which means that they start living at the seabed of the Barents
74 Sea (Jakobsen and Ozhigin, 2011, page 228-230). The trawlers target shrimps at the
75 seabed and it is therefore reasonable to believe that the amount of bycatch within the
76 shrimp fishery industry is related to the abundance of 0-group fish within the area. As
77 far as we know there has been no statistical research on such a connection before.

78 The results in this paper can help MSS to optimize their resource allocation and improve
79 their decision making, and make short time future fishing grounds more predictable for
80 the fishermen. The model proposed can easily be extended to prediction of bycatch for
81 other species and to other fisheries. The model can also be combined with many types of
82 random effects as well as observation models (e.g. zero-inflated models as suggested by
83 Aldrin et al., 2012).

84 **Data**

85 We used 7363 observations of shrimp trawl hauls from 1994 to 2006 provided by the
86 Institute of Marine Research (IMR) in Bergen, Norway. Originally we were given 7420
87 observations of shrimp catch and bycatch that were also used to predict bycatch ratios
88 in Aldrin et al. (2012). But after a thorough study of the data, we discarded 57 observa-
89 tions and further corrected 14 observations of shrimp catches that were wrongly given in
90 kilogram instead of ton. See Fig. 1 for an illustration of the locations of the observations
91 and Table 1 for a short summary of the data. In the data there were 5419 observations
92 with a single trawl, 1727 with a double trawl and 217 with a triple trawl. Approximately
93 a fifth of the observations lack information about the circumference of the trawl. For
94 these observations, which had only simple and double trawls, we fixed the circumference

95 to the average number of meshes around the opening within the type of trawl, that is
96 2200 meshes for a single trawl and 2480 meshes for a double trawl. There were 18.6 %
97 zeroes in the bycatch data, and most of them were in the summer when we should often
98 expect low bycatch.

99 Every late summer, around August/September, IMR and the Polar Research Institute
100 of Marine Fisheries and Oceanography (PINRO) in Murmansk, Russia, cooperate to es-
101 timate 0-group abundance. These estimates were calculated by a standard procedure:
102 Short trawls, each 0.5 nautical mile, were taken at three or more depths with head-line at
103 0, 20 m, 40 m, and so on. The number of cod caught was then corrected with a capture
104 efficiency function of cod length, and scaled up to make an estimate of the 0-group abun-
105 dance per square nautical mile (Eriksen et al., 2009). Fig. 2 shows the spatial locations of
106 the 0-group estimates in four different years. The number of estimates (spatial locations)
107 varied from 230 to 400 in the period 1993 to 2006 which means we had detailed informa-
108 tion about where the 0-group individuals were located in August/September.

109 Models

110 The Bayesian hierarchical model contains two main sub-models, one for catch of shrimps
111 (kg) and one for bycatch (counts). Let $C(\mathbf{s}, t)$ be kilogram shrimp caught at time t and
112 location \mathbf{s} , scaled to be per nautical mile, and set $Z(\mathbf{s}, t) = \log(C(\mathbf{s}, t))$. The model for
113 the shrimp catch is defined as

$$Z(\mathbf{s}, t) = \mathbf{X}_Z(\mathbf{s}, t)\boldsymbol{\beta}_Z + \alpha_Z(\mathbf{s}) + v_Z(t) + \gamma_Z(\mathbf{s}, t) + \epsilon_Z(\mathbf{s}, t). \quad (1)$$

114 Here $\mathbf{X}_Z(\mathbf{s}, t)$ is a vector of covariates (e.g. seasonal effect and gear equipment) and
115 $\boldsymbol{\beta}_Z$ is the corresponding vector of regression coefficients. Three random effect terms are
116 included; the spatial random field, $\alpha_Z(\mathbf{s})$, is intended to capture that the amount of

117 shrimps might depend on local features, e.g. shrimps are known to be located at frontal
 118 zone areas (Jakobsen and Ozhigin, 2011, page 173). The temporal random field, $v_Z(t)$,
 119 is intended to capture that catches change over time. The spatio-temporal random field,
 120 $\gamma_Z(\mathbf{s}, t)$, is intended to capture that observations close in both space and time are probably
 121 more equal. All these random effects are modeled as Gaussian fields with dependence
 122 structures defined through covariance functions. Finally, $\epsilon_Z(\mathbf{s}, t)$ describes measurement
 123 noise or micro-scale variability.

124 We assume a similar model for the bycatch. Let $B(\mathbf{s}, t)$ be the number of juvenile
 125 cod caught at time t and location \mathbf{s} , scaled to be per nautical mile, and set $Y(\mathbf{s}, t) =$
 126 $\log(B(\mathbf{s}, t) + 1)$. Our model for the bycatch is defined as

$$Y(\mathbf{s}, t) = \mathbf{X}_Y(\mathbf{s}, t)\boldsymbol{\beta}_Y + \alpha_Y(\mathbf{s}) + v_Y(t) + \gamma_Y(\mathbf{s}, t) + \epsilon_Y(\mathbf{s}, t), \quad (2)$$

127 where the interpretation of the terms involved are similar to model (1). The covariates
 128 that have been considered are given in Table 2. The 0-group abundance and shrimp catch
 129 covariate in Table 2 are only used in the bycatch model (2). Alternative models such as
 130 Poisson, negative binomial and a zero-inflated negative binomial distribution have also
 131 been considered, but they did not perform as well as the log-Gaussian distribution, see
 132 further comments on this in the discussion section.

133 The seasonal effect included requires some further discussion. We used a Fourier se-
 134 ries (Lay, 2006, page 456) for the seasonal effect. The Fourier series is given by

$$f(t') = \sum_{i=1}^r (c_i \sin(it') + d_i \cos(it')), \quad (3)$$

135 were $t' \in [0, 2\pi]$ with $t'(1\text{st January}) = 0$, $t'(31\text{st December}) = 2\pi$ and linear in time.
 136 Here c_i and d_i correspond to regression coefficients within equations (1) and (2). Fourier

137 series are used since the seasonal effect should be the same at the start and the end of
138 the year, and because seasonal effects typically have a harmonic pattern.

139 The growth rate of the cod depends on the temperature (Jørgensen, 1992), and the
140 time at which a 0-group cod changes to a demersal life phase might depend on its size.
141 We therefore allow the seasonal effect to be a function of latitude since it is typically
142 colder in the north. This is implemented in the model by first assuming two different
143 Fourier series (3), one at the northernmost location point containing data and another
144 at the southernmost location point. Seasonal effects at other locations are then defined
145 to be convex combinations of the seasonal effects in these two points. The weights in
146 the convex combination are chosen to range from 0 to 1 and to be linear in the vertical
147 distance between the location and the northernmost and southernmost point.

148 **Spatial, temporal, and spatio-temporal Gaussian random fields**

149 We included three correlation structures in our models (1) and (2) via Gaussian random
150 fields, one spatial, one temporal and one spatio-temporal. This section describes the
151 correlation structures for the Gaussian random fields involved in models (1) and (2).
152 For brevity we will not use the subheadings Z and Y when elaborating the correlation
153 functions.

154 We assume that the spatially correlated Gaussian field, $\alpha(\mathbf{s})$, has zero mean and follows
155 the stationary Matern covariance function (Stein, 1999) given by:

$$\text{Cov}(\alpha(\mathbf{s}_1), \alpha(\mathbf{s}_2)) = \frac{\sigma_\alpha^2}{2^{\nu-1}\Gamma(\nu)} (\kappa \|\mathbf{s}_1 - \mathbf{s}_2\|)^\nu K_\nu(\kappa \|\mathbf{s}_1 - \mathbf{s}_2\|), \quad (4)$$

156 where σ_α^2 is the marginal variance, ν is a smoothing parameter, κ is a spatial scale
157 parameter, $\|\mathbf{s}_1 - \mathbf{s}_2\|$ is the distance between \mathbf{s}_1 and \mathbf{s}_2 in kilometers and $K_\nu(\cdot)$ is the
158 modified Bessel function of the second kind. In this study we fixed $\nu = 1$ since this

159 value is implemented in the R-INLA package and since the value of ν is typically poorly
160 identifiable (Blangiardo and Cameletti, 2015, page 194).

161 We assume the time-dependent zero-mean Gaussian random field, $v(t)$, to be constant
162 within years while independent between years, with variance σ_v^2 . An AR(1)-structure in
163 the yearly effect was also investigated, but this extra structure was not supported by
164 data. It is important to note that we define the first month of the year to be September
165 when we refer to a yearly effect in the bycatch model. This is reasonable because in
166 September/October the 0-group starts entering a demersal life stage, and thereby starts
167 living on depths where shrimp trawling occurs (Jakobsen and Ozhigin, 2011, page 230).
168 In the shrimp model, the year starts in January.

169 For the spatio-temporal interaction term, $\gamma(\mathbf{s}, t)$, we assume a stationary zero-mean Gaus-
170 sian field with a separable covariance function. We test three different, but quite similar
171 covariance functions. The first two are given by

$$\text{cov}\left(\gamma(\mathbf{s}_1, t_1), \gamma(\mathbf{s}_2, t_2)\right) = \sigma_\gamma^2 \exp\left(-\frac{\|\mathbf{s}_1 - \mathbf{s}_2\|^q}{\theta_s} - \frac{|t_1 - t_2|}{\theta_t}\right) \quad (5)$$

172 with $q = 1$ or 2 . Here $\|\mathbf{s}_1 - \mathbf{s}_2\|$ is the distance between \mathbf{s}_1 and \mathbf{s}_2 in kilometers, $|t_1 - t_2|$
173 is the time difference in days and θ_s and θ_t describe the correlation lengths in space and
174 time. Both $q = 1$ and $q = 2$ give special cases of the Matern covariance function (4) as
175 the spatial contribution to the separable spatio-temporal interaction (5), the first with
176 $\nu = 0.5$ and the second with $\nu = \infty$ (Minasny and McBratney, 2005).

177 The third covariance function considered was introduced within the R-INLA framework
178 by Cameletti et al. (2013) and also tested (but rejected) in Cosandey-Godin et al. (2014).
179 In this case the covariance function is indirectly defined through the introduction of a
180 spatial grid overlapping the area of interest and a dynamic model for changes between

181 time points:

$$\boldsymbol{\xi}_r = a\boldsymbol{\xi}_{r-1} + \boldsymbol{\omega}_r, \quad \boldsymbol{\omega}_r \sim N(\mathbf{0}, \tilde{\boldsymbol{\Sigma}}) \quad r = 1, \dots, T. \quad (6)$$

182 Here $\boldsymbol{\xi}_r = (\xi(\mathbf{s}_1, r), \dots, \xi(\mathbf{s}_d, r))$ are the values of the spatio-temporal process at time
183 point r and grid points $\mathbf{s}_1, \dots, \mathbf{s}_d$, a is an unknown autoregressive parameter and $\boldsymbol{\xi}_0 \sim$
184 $N(\mathbf{0}, \tilde{\boldsymbol{\Sigma}}/(1 - a^2))$. The covariance matrix $\tilde{\boldsymbol{\Sigma}}$ is specified such that it approximates a
185 Matern covariance matrix in space for the d spatial grid points with $\nu = 1$ (see Cameletti
186 et al., 2013, for further details).

187 Notice that the covariance structures in (5) and (6) are almost identical, except that in (6)
188 we discretize time and approximate the Matern covariance function (4) with $\nu = 1$ as the
189 spatial contribution to the separable spatio-temporal interaction. See the appendix for a
190 detailed derivation of this.

191 Predictions of bycatch ratio for management

192 The bycatch ratio in an area A at time t is defined by (Ye, 2002):

$$R_{A,t} = \frac{\sum_{\mathbf{s} \in A} \text{Bycatch}(\mathbf{s}, t)}{\sum_{\mathbf{s} \in A} \text{Target catch}(\mathbf{s}, t)}, \quad (7)$$

193 where $\text{Bycatch}(\mathbf{s}, t)$ is the number of juvenile cod caught in a trawl haul at location \mathbf{s} at
194 time t , and $\text{Target catch}(\mathbf{s}, t)$ is the kilogram of shrimp caught. The bycatch ratio (7)
195 can be interpreted as the total bycatch ratio over a large number of hypothetical trawls
196 taken in area A at time t .

197 The bycatch ratio (7) in an area A at time t is predicted as in Aldrin et al. (2012) by
198 Monte Carlo estimation:

$$\hat{R}_{A,t} = \frac{1}{N} \sum_{i=1}^N \frac{\sum_{g=1}^G B^i(\mathbf{s}_g, t)}{\sum_{g=1}^G C^i(\mathbf{s}_g, t)}. \quad (8)$$

199 Here the outer sum is the Monte Carlo estimation, the inner sums approximate the sums
 200 in (7) where $\{\mathbf{s}_1, \dots, \mathbf{s}_G\}$ is a sufficiently dense set of spatial grid points in A . Here it is
 201 important that N must be large to encounter the uncertainty in $\hat{R}_{A,t}$, and G must be
 202 large to ensure that the estimated bycatch ratio can be interpreted as the total bycatch
 203 ratio over a large number of hypothetical trawls. We used $N = 2000$ and found $G \approx 200$
 204 appropriate in our application.

205 In our research we have seen that the magnitude of the seasonal effect on shrimp catch
 206 and the spatio-temporal correlation parameters varies in space and therefore we only
 207 used observations relatively close to the center of the area of interest when predicting the
 208 bycatch ratio (7). In our application the areas are typically defined by a few vertices,
 209 and the center of the area we define as the point with shortest sum of distances to all
 210 the vertices defining the area. To obtain the bycatch ratio predictions we only used
 211 observations closer than 600 km from the center of the area of interest. We expect that
 212 these observations are enough for making a good prediction and that we gain by excluding
 213 observations far away in space because of the more accurate estimation of the magnitude
 214 of the seasonal effect of shrimp catch and range of the spatio-temporal correlation in the
 215 area of interest.

216 Inference

217 The models for shrimp catch (1) and bycatch (2) are general additive latent Gaussian, and
 218 efficient computation can thereby be performed through the R-package R-INLA ([http:](http://www.r-inla.org)
 219 [//www.r-inla.org](http://www.r-inla.org), Rue et al., 2009, Martins et al., 2013). We have always used default
 220 priors (who are reasonably non-informative, see details in the appendix), and thereby let

221 the 7363 observations inform the posterior distributions.

222 For computationally efficiency we approximate the spatial Gaussian fields, $\alpha^Z(\mathbf{s})$ and
223 $\alpha^Y(\mathbf{s})$ in equation (1) and (2), with Markov random fields. The approximation method
224 used is explained in Lindgren et al. (2011) and is based on that the Matern covariance
225 function (4) is a solution of a stochastic partial differential equation (SPDE). This solution
226 can be approximately represented by a Markov random field with a sparse precision matrix
227 which makes it possible to apply fast Laplace approximations (Rue et al., 2009).

228 Since we approximate the spatial Gaussian field with a Markov random field we need to
229 define a spatial grid, this grid is shown in Fig. 3. Such triangulation based grids are easy
230 to create in the R-INLA package and have several clear advantages compared to regular
231 square grids. To make the Markov random field approximation continuous we further let
232 the value at each point in the domain (that is not a vertex) be a convex combination of the
233 estimated values at the three vertices defining a triangle around it (Lindgren et al., 2011).
234 Many of the observations are very close in space. In order not to make the triangulation
235 very dense, we have chosen the triangulation such that no edges are closer than 20 km
236 from each other. This has negligible effect on the results and it speeds up the calculations
237 compared to letting each observation location be a vertex.

238 The covariance structure for the spatio-temporal effects defined in (5) is currently not
239 directly available in R-INLA. However, a generic class is available where the *precision*
240 *matrix* is given by $\mathbf{Q} = \tau\mathbf{C}$ where τ^{-1} is the marginal variance and \mathbf{C} is fully specified.
241 In our case \mathbf{C} is a function of the parameters θ_s and θ_t in (5) resulting in that R-INLA can
242 only be applied for prespecified values of these parameters. By running R-INLA several
243 times and maximizing the marginal likelihood, posterior modes for θ_s and θ_t are obtained.
244 In this research we only used the posterior mode of θ_s and θ_t and thereby neglected the
245 uncertainty in these two parameters. To do fast approximation, R-INLA further requires
246 sparse precision matrices. We made the precision matrix sparse by truncating to zero all
247 elements in \mathbf{C} that are less than 0.01 and are referring to locations more than one range
248 unit away from each other. The range is here defined as the distance in time and space

249 with correlation equal to 0.1. We tried different small thresholds for setting the elements
250 \mathbf{C} to zero, and the differences of the results were negligible.

251 Consider now the spatio-temporal correlation structure introduced in Cameletti et al.
252 (2013), see equation (6). A problem in using this correlation structure for our data is
253 that the observations are unstructured in space and time. To use this approach we need to
254 discretize time and define a spatial grid approximation also for this part of the model (6).
255 For computational reasons, a very coarse spatial as well as temporal discretization is
256 needed. We chose to discretize time in intervals of 30 days, and used a spatial mesh with
257 346 edges and with no edges closer than 50 km from each other.

258 **Model selection**

259 For model selection, we used the procedure recommended in Zuur (2009, page 121) where
260 first the correlation structures are specified (through selection of which of the three ran-
261 dom effects that should be included), using all relevant covariates, followed by a selection
262 of significant covariates using the selected correlation structure.

263 We used four methods when evaluating correlation structures: Bayes factor (Gelfand,
264 1996), pseudo-Bayes factor (Gelfand, 1996), the DIC-value (Spiegelhalter et al., 2002)
265 and mean square error (MSE) of the observed values compared with the expected value
266 of (1) and (2), respectively. The Bayes factor is the ratio of the marginal likelihoods
267 (ML) from a pair of models. The pseudo-Bayes factor is the ratio of the cross-validation
268 densities (CVD) given by $CVD = \prod_{i=1}^n P(y_i | \mathbf{y}_{-i}, M)$, where \mathbf{y}_{-i} are all the observations
269 except y_i and M represents the model. See Rue et al. (2009) on how the ML and
270 CVD are calculated within R-INLA. When calculating the MSE we remove every tenth
271 observation and predict these, this we repeat ten times until we have predictions for all
272 the observations. We used the Bayes factor for backward elimination of covariates.

273 Computational features

274 The research was done on a computer with Intel Core i5-2500 CPU 3.30GHz \times 4 processor,
275 and R-INLA utilizes all the four cores. With the 7363 observations the calculations took
276 about 16 minutes for the final bycatch model and five minutes for the final shrimp catch
277 model after the posterior mode of the spatio-temporal parameters θ_s and θ_t (eq (5)) was
278 found.

279 Results

280 The results section is divided into three parts: 1) covariates, 2) covariance structure, and
281 3) model performance with regards to decision making on time/area closures compared
282 to previous models in this fishery (Aldrin et al., 2012).

283 Covariates

284 Table 3 lists the covariates that were selected for the prediction of shrimp and bycatch.
285 For the description of the seasonal effects (3) we included one harmonic term in the
286 shrimp model, and three harmonic terms in the bycatch model. The seasonal effect of
287 bycatch varied in space, the further north the later the seasonal effect will increase in late
288 fall/early winter. See Fig. 4 for illustration of the seasonal effects.

289 By looking at credibility intervals, we found a clear effect of the strength of the 0-group
290 of cod in the Barents Sea on the bycatch when aggregating the 0-group estimates over
291 space, see Table 3. Our model predicts that if the 0-group abundance doubles, the
292 bycatch increases by approximately 29% with 95% credibility interval (13%, 47%). The
293 Bayesian factor was indifferent to the inclusion of the 0-group when the yearly effect was
294 included, but the inclusion of the 0-group halved the variance of the year effect, giving
295 better predictive power when included. We therefore decided to include this effect into

296 the model.

297 The more shrimp that is caught, the more bycatch we can expect. If we double the shrimp
298 catch the bycatch increases with approximately 18% (16%, 21%). In times of the year
299 when there is neither midnight sun nor polar nights the model predicts that it is much
300 harder to catch shrimp and we get less bycatch in the night. The size of the coefficients
301 implies that the shrimp catch reduces with 34% (27%, 41%), and the bycatch reduces
302 with 23% (11%, 33%). Since both the bycatch and the shrimp catch decrease during
303 night time trawling, this variable has lesser effect on the bycatch ratio. In time of the
304 year when there is midnight sun or polar nights we found no night effect.

305 The model found that larger equipment often leads to larger catch. Compared to using
306 a single trawl, the model predicts that the shrimp catch increases by 80% (67% , 95%)
307 if we use a double trawl and 222% (153%, 306%) if we use a triple trawl. We have
308 few observations with triple trawls, which might explain the large uncertainty of this
309 coefficient. The bycatch is predicted to increase by 32% (17%, 48%) if we use a double
310 trawl while we did not find any increase by using a triple trawl. That triple trawls have
311 no effect on the bycatch we think is intuitively surprising, the reason might be that the
312 shape of the trawl differs when several trawls are used or that we do not have enough
313 observations with triple trawls.

314 **Covariance structure**

315 When considering model selection with respect to the covariance structure (random ef-
316 fects), both the shrimp and bycatch models, including spatio-temporal correlation struc-
317 ture given by (5) with $q = 1$, were clearly favored, see Table 4. The optimal shrimp catch
318 model contains only a spatial and a spatio-temporal interaction term in (1). The optimal
319 bycatch model includes a spatial, a temporal as well as a spatio-temporal interaction term
320 in (2).

321 Table 5 shows the values of the parameters in the correlation structure in the final model
322 while Fig. 5 shows the spatial effects of the bycatch and the shrimp catch. The ranges
323 in space and time in the spatio-temporal Gaussian fields (5) are estimated to be ap-
324 proximately 160 days and 150 km for the shrimp catch and 90 days and 310 km for the
325 bycatch.

326 From the estimated mean of the marginal variances in Table 5 we can interpret how the
327 variation in the observations are distributed among the random terms in (1) and (2). We
328 see that most of the variation was in the spatial part, secondly in the spatio-temporal
329 part, thirdly in the unstructured part and least in the temporal part. Note that, as stated
330 above, the latter part is only included in the optimal bycatch model.

331 **Decision making**

332 In this section we illustrate how the model performs with respect to the important decision
333 of whether to open or close an area for shrimp fishing. Remember that an area should
334 be closed if the bycatch ratio (7) is expected to exceed 0.8 cod per kilogram shrimp. We
335 predict the bycatch ratio (7) through (8). In this section we first investigate how well the
336 model performs in a certain area where there is much shrimp catch activity. Then we
337 investigate more generally how good the model predicts bycatch ratios when using parts
338 of the observations from MSS as test sets.

339 As in Aldrin et al. (2012), we predicted the bycatch ratio at 1st of December 2005 in
340 the Hopen area. See Fig. 1 for an illustration of the Hopen area. At that time an
341 inspector from MSS was investigating 21 trawl hauls in the Hopen area on a boat with a
342 single trawl with 3600 meshes around the opening. Our predictions of bycatch are done
343 by taking the fishing gear equipment into account, while Aldrin et al. (2012) did not
344 consider such an effect. We first predicted the bycatch ratio at 1st of December 2005
345 based only on observations previous to that date. Thereafter we updated the prediction
346 while sequentially including 1,3,5,10,15 and 21 additional observations sorted in the order

347 they were taken in the period 3rd to 6th of December 2005. The predictions and credibility
348 intervals of the bycatch ratio are given in Table 6, the predictions by the model currently
349 in use is referred to as the simple model. Confidence intervals of the simple bycatch ratio
350 estimates are calculated by using nonparametric bootstrapping (Efron and Tibshirani,
351 1994).

352 We used $G = 203$ in equation (8) when estimating the bycatch ratio in this area, and
353 we observed that using a larger G changed the estimates negligibly. Furthermore, the
354 restriction to only use observations closer than 600 km from the center of the area of
355 interest resulted in that we used 4784 observations before 1st of December 2005.

356 With the regulation method used today, predictions without any recent observations
357 are not possible and MSS needs to take many new (expensive) observations to obtain
358 reliable results. From Table 6 we see that both our model and the model introduced
359 in Aldrin et al. (2012) are able to do reasonable predictions even with very few recent
360 observations within the area of interest. Furthermore, our predictions are quite close to
361 the predictions given in Aldrin et al. (2012). This is not surprising since we concluded
362 to use a quite similar model. The new model is however able to detect a bycatch ratio
363 that is significantly higher than 0.8 in more cases with few observations compared to the
364 model in Aldrin et al. (2012).

365 The results clearly indicate that the Hopen area should be closed in the beginning of
366 December 2005. The next decision problem then is when to open again. Our model can,
367 even without extra samples, predict bycatch ratios at any time. Fig. 6 illustrates the
368 predicted bycatch ratios after December 2005 given only the observations up to Decem-
369 ber 6. These results indicate that the area could be opened for shrimp fishing in April
370 2006.

371 We predicted the bycatch ratio in several other periods and locations, with promising
372 results. We illustrate one such set of predictions for bycatch ratios. In 2005 and 2006
373 there were 18 months with trawl haul observations in the Hopen area. Fig. 7 shows the

374 bycatch ratio predictions of the trawl hauls for each month in that period using only
375 observations previous to the beginning of the month. From Fig. 7 we see that the model
376 is able to give realistic predictions of the bycatch ratios compared to the observed bycatch
377 ratios. Notice that the predicted bycatch ratio in December 2005 and November 2006
378 clearly differed from the observed bycatch ratio. This was because of very low shrimp
379 catches that resulted in a high bycatch ratio. The reason for a slightly difference between
380 ratio prediction in June 2006 and the observed bycatch ratio is discussed in the discussion
381 section.

382 We also investigated how well the bycatch ratio estimation performed when using parts
383 of the observations from MSS as test sets. We defined a test set by sequentially selecting
384 every tenth trawl haul in the data. For these hauls, point predictions together with
385 90% and 99% prediction intervals for bycatch ratios were calculated. By comparing the
386 prediction intervals with the true observations we were able to investigate the coverage.
387 From Table 7 we see that the prediction intervals have roughly the right coverage. The
388 90% prediction intervals seemed to have the right coverage for bycatch and shrimp catch,
389 but when looking at the extremes, the 99% prediction intervals seemed to have slightly
390 less coverage. The largest difference is that the model too often failed to predict small
391 shrimp catches, but in a regulation perspective this is not a very important error since
392 low shrimp catches lead to small commercial shrimp catch activity.

393 Discussion

394 The objective of this paper was to construct statistical rigid models for shrimp catch
395 and bycatch that can be used to regulate the shrimp fishery with respect to bycatch.
396 This discussion is divided in four parts: The first part is about the covariates and the
397 covariance structures. The second part is about alternative observation models. The
398 third part is elaborating comparisons with earlier research (Aldrin et al., 2012). The
399 fourth and final part is about how the methodology introduced in this paper can be used

400 by the MSS and in other biological applications.

401 **Covariates and correlation**

402 Fig. 5 shows the spatial effects of the bycatch and the shrimp catch. The spatial structure
403 for bycatch looks very intuitive since the cod spawn mainly in the north of Norway and
404 the larvae drift passively in the upper layers with the currents into the Barents Sea. In
405 August/September the juvenile cod are distributed at most places at the warm side of
406 the Polar Front with typically largest concentration in the central Barents Sea (Jakobsen
407 and Ozhigin, 2011, page 230).

408 Fig. 4a and 4b illustrate the seasonal effects for the bycatch. The increase in Septem-
409 ber/October is caused by the 0-group entering a demersal phase. The model predicts
410 that a cod changes to a demersal phase later in the north (Hopen) compared to the
411 south (Lyngen). This is reasonable since the cod grows slower in the cold water far
412 north (Jørgensen, 1992).

413 From Fig. 4c we also see that the model predicts higher shrimp catches in late spring
414 compared to the winter. This is probably due to the shrimps vertical migration pattern
415 which is dependent on light conditions (Hopkins et al., 1993). By estimating the seasonal
416 effect of shrimp catch at different areas (not shown), we noticed that the shape of the
417 seasonal effect is the same but the magnitude seems to depend on the location. We tried
418 to account for this interaction between space and seasonal effect, similar to what we did
419 for bycatch, but there was no support in the data for including this into the model.

420 We tried to utilize the spatial locations of the estimates of the 0-group as a possible *spatial*
421 predictor for bycatch by using estimates of the number of cod per square nautical mile in
422 areas around the bycatch observations, but data did not support to include this into the
423 model. We therefore concluded only to use the estimated total number of 0-group of cod
424 present in the Barents Sea. These estimates can be found in Jakobsen and Ozhigin (2011,

425 page 565) and are calculated by the same 0-group data as used in this work. We believe
426 that there are two main reasons for not being able to utilize the spatial locations of the
427 estimates of the 0-group. One reason is that the cod can drift a long distance with the
428 currents before it changes to a demersal life phase later that year. The other reason is that
429 the amount of cod per nautical mile estimated as in Eriksen et al. (2009) at each location
430 has a very large, and difficult to quantify, variance. Therefore few observations might give
431 little information, while spatial aggregation of the 0-group gives more reliable covariates.
432 To better encounter that the 0-group changes from year to year, we have in addition tried
433 to include a Gaussian field with a correlation structure given as in Cameletti et al. (2013),
434 see equation (6), with time discretized as yearly intervals lasting from 1st of September to
435 31th of August. By visually inspecting the yearly spatial-temporal contributions we have
436 seen no clear correspondence with the yearly spatially distribution of the 0-group given
437 in Jakobsen and Ozhigin (2011, 564). Adding such a correlation structure was neither
438 supported by data based on our validation methods.

439 Because of our noninformative priors, and the confounding between the yearly effect and
440 the 0-group, the Bayes factor equally favored bycatch models with and without the 0-
441 group (when the yearly effect was included). However, including the 0-group covariate
442 resulted in a large decrease (from 0.44 to 0.2) in the variability of the year effect, resulting
443 in higher predictive power from a management perspective. Because of this we included
444 this covariate as well.

445 The amount of shrimp catch was clearly important for the bycatch, even when scaled
446 by distance. This might be because the shrimp and cod feed on the same prey and
447 thereby might be concentrated at the same locations. The night effect was clearly an
448 important covariate for both the bycatch and the shrimp catch. This might be explained
449 by the shrimps being known to feed on pelagic prey species especially at night and hence
450 stay semi pelagic above the trawl gear during night (Jakobsen and Ozhigin, 2011, page
451 176).

452 We both included a pure spatial field and a spatio-temporal random field in the models.

453 The spatial Gaussian field is intended to capture that some places are expected to have
454 small or large catches due to biological or geophysical features. Inclusion of a pure spatial
455 field resulted in a spatio-temporal field with a much smaller spatial and temporal range
456 than a model without a spatial field. Our model is aimed for predicting sudden changes
457 in the bycatch, and thereby be able to help the MSS to open or close areas. Therefore
458 we need a correlation structure that can detect sudden changes. We believe we managed
459 this in a satisfactory manner. A reason for this is that when including a pure spatial
460 Gaussian field we are able to include a spatio-temporal structure that can only focus
461 on the local changes in time and space. As opposed to previous research (Cosandey-
462 Godin et al., 2014), we concluded to use the continuous correlation structure (5) for the
463 spatio-temporal field in order to take into account the structure in the observations.

464 **Observation models**

465 In addition to the log-Gaussian distribution for the observations in the bycatch model,
466 we also considered Poisson, Negative Binomial and zero-inflated Negative Binomial dis-
467 tribution. We considered a zero-inflated distribution in R-INLA (<http://www.r-inla.org>)
468 which allows the zero-probability to decrease when the expectation increases because we
469 believe this is reasonable in our application. Of the alternative distributions, the Negative
470 Binomial distribution gave the best fit to the data. When comparing the Negative Bino-
471 mial distribution with the log-Gaussian distribution, the log-Gaussian distribution gave
472 more accurate predictions (when comparing the sum of absolute errors of the number of
473 cod taken as bycatch). The histogram of Bayesian p-values (Gelman et al., 2003) looked
474 more uniform when using a log-Gaussian distribution. The pseudo-Bayes factor also gave
475 preference to the log-Gaussian distribution. Because of this we chose the log-Gaussian
476 distribution. In Cosandey-Godin et al. (2014) the authors used a latent Gaussian model
477 with zero-inflated negative binomial distribution to estimate bycatch of Greenland shark
478 in the Greenland Halibut fishery. In their application the bycatch values were low (mostly
479 zero). In our application, with many large bycatch-numbers, the log-Gaussian distribu-

480 tion is more appropriate.

481 There are cases of extremely large observations of bycatch in the summer when the
482 model predicts little bycatch. This is probably because marine resources often are highly
483 patchy (Seber, 1986) and the trawler has trawled through a large school of juvenile cod.
484 One example of this we see in July 2006 (Fig. 7) were one haul contained 616 juvenile
485 cod per distance (compared to (2, 92) cod per distance in the other hauls). Such a
486 large bycatch in one trawl is not normal in the summer and gave, with our model, a
487 Bayesian p-value (Gelman et al., 2003, page 162) approximately equal to 0.0005. This
488 one trawl haul then resulted in the Bayesian p-value of the total bycatch ratio that month
489 (consisting of 9 trawl hauls) became approximately 0.02. We tried to use a *t*-distribution
490 for the observations within the bycatch model to partly encounter for this scenario, but
491 then the degree of freedom was estimated to be 18, and thereby there was little difference
492 compared to the Gaussian distribution.

493 **Comparison with Aldrin et al. (2012)**

494 The model introduced in this research is an extension of the model introduced in Aldrin
495 et al. (2012). In that paper the authors introduced an additive regression model for
496 shrimp catch and bycatch and first estimated the regression parameters with the least
497 square method. Then they estimated the hyperparameters in the correlation structure
498 given the regression parameters with a maximum likelihood method (they only used
499 three parameters in the correlation structure since they did not use the very important
500 yearly effect on bycatch and used a spline method for the spatial effect). To estimate
501 the correlation structure in reasonable time, Aldrin et al. (2012) further divided the
502 observations into 24 segments in time and space and assumed independence between
503 segments. In our approach we find the posterior distribution for all the parameters
504 simultaneously and thereby make the method more rigid. We are able to do this because
505 the R-INLA package effectively calculates the posterior distributions.

506 Aldrin et al. (2012) stated that considering the Negative Binomial distribution would be
507 interesting in further work. R-INLA allows to easily consider different distributions for
508 the observations. In the R-code we only need to change a few lines to let the R-INLA
509 package run with another distribution (<http://www.r-inla.org>).

510 A problem encountered and efficiently dealt with in Aldrin et al. (2012) was that the
511 variance of the residuals depended on the expectation. We did not encounter this problem
512 within our model. This may be because we scaled the response by the distance trawled,
513 and thereby accommodate for external factors that might explain the heterogeneity that
514 was present in the Aldrin et al. (2012) model.

515 **Practical implications of the model**

516 The MSS has limited resources and needs to optimize the choice of locations to collect
517 observations for predicting the bycatch ratio. The model introduced in Aldrin et al. (2012)
518 and further extended in this research can help MSS to optimize the use of observations
519 and thereby the collection of data within their resource limits. Our method predicted
520 the bycatch ratio to be high enough to close the Hopen area for shrimp fishing in early
521 December 2005. Without the need for further observations, our method also predicted
522 that the area could be opened in April 2006 (see Fig. 6), thereby saving the cost of
523 collecting expensive new observations.

524 The model introduced can also be used to predict the historical total bycatch in shrimp
525 fishery. Historical total bycatch prediction has previously often been performed by scaling
526 up the observed bycatch ratio in areas with the commercial shrimp catch (Ye, 2002,
527 Ye et al., 2000, Davies et al., 2009, Amandè et al., 2010). We expect that the model
528 introduced in this research will give more reliable estimates of the total bycatch, including
529 uncertainty. There is ongoing work to predict the historical bycatch of cod, redfish and
530 haddock in the Barents Sea shrimp fishery by using the model introduced here.

531 Acknowledgments

532 The authors want to thank Frank Kristoffersen (inspector at MSS) and Erik-Andre Brose
533 Krag (captain on a shrimp trawler) for valuable discussions lasting four days while the
534 first author was on an expedition in Lyngen trawling for shrimps. The authors also
535 want to thank Sondre Aanes, Jørund Gåsemøy, Bent Natvig and Ida Scheel for valuable
536 discussions of the model and comments, statistics for innovation (SFI²) for funding and
537 PINRO for allowing the authors to use the observations of the 0-group of cod. The
538 authors are also very thankful for comments from two anonymous reviewers which led to
539 a much improved article.

540 Appendix

541 Night effect

542 The night effect has been observed by fishermen to be particularly strong in the time of the year
543 when there is neither midnight sun nor polar nights. To accommodate for the night effect we
544 thereby distinguished between two periods in the year named the *transient period* and the *sta-*
545 *tionary period*. The stationary period was defined as the period where there was either midnight
546 sun or polar night, and the transient period was defined as the complement of the stationary
547 period. We then introduced two indicator variables, one defines the transient/stationary period,
548 and another defines day/night. To define the stationary period (and thereby also the transient
549 period) we defined five reference points in the Barents Sea and adjunct waters where we know the
550 stationary period (<http://www.yr.no>). The five reference points are: Rossøya (80.8°N), Hopen
551 (76.5°N), Bjørnøya (74.5°N), Nordkapp (71.2°N) and Tromsø (69.6°N). We then approximated
552 the stationary period in a location to be the same as in the closest reference point in latitude
553 direction. Furthermore, we define that the trawl was done at night if the trawler started after 9
554 pm or ended in the period between midnight and 9 am.

555 Correlation

556 We now illustrate the similarities stated between the spatio-temporal interaction correlation
 557 structures (5) and (6). Let $k > 0$ be an integer. We have from (6) that:

$$\begin{aligned}
 \text{cov}\left(\xi(\mathbf{s}_1, r), \xi(\mathbf{s}_2, r + k)\right) &= \text{cov}\left(\xi(\mathbf{s}_1, r), a\xi(\mathbf{s}_2, r + k - 1) + \omega_{r+k}(\mathbf{s}_2)\right) \\
 &= a\text{cov}\left(\xi(\mathbf{s}_1, r), \xi(\mathbf{s}_2, r + k - 1)\right) \\
 &= a^k \text{cov}\left(\xi(\mathbf{s}_1, r), \xi(\mathbf{s}_2, r)\right) \\
 &= \sigma_\omega^2 \exp\left(\ln(C(\|\mathbf{s}_1 - \mathbf{s}_2\|)) + k \ln(a)\right), \tag{9}
 \end{aligned}$$

558 where $C(\cdot)$ is the Matern correlation function with $\nu = 1$, σ_ω^2 is the marginal variance of the
 559 corresponding Matern covariance function and $\|\mathbf{s}_1 - \mathbf{s}_2\|$ is the distance between \mathbf{s}_1 and \mathbf{s}_2 in
 560 kilometers. The similarities stated between (5) and (6) are now easily seen.

561 Priors

562 The noninformative priors for the hyperparameters used in this research are given in Table 8.
 563 The gamma distribution used has the parametrization:

$$\pi(x|\alpha, \beta) = \frac{\beta^\alpha}{\Gamma(\alpha)} x^{\alpha-1} \exp(-\beta x). \tag{10}$$

564 INLA by default uses an improper prior for the intersect regression coefficient and a $N(0, 1000)$
 565 prior for the other regression coefficients.

References

- 566 Aldrin, M., Mortensen, B., Storvik, G., Nedreaas, K., Aglen, A. and Aanes, S. (2012),
567 ‘Improving management decisions by predicting fish bycatch in the Barents Sea shrimp
568 fishery’, *ICES Journal of Marine Science: Journal du Conseil* **69**(1), 64–74.
569
- 570 Amandè, M. J., Ariz, J., Chassot, E., De Molina, A. D., Gaertner, D., Murua, H.,
571 Pianet, R., Ruiz, J. and Chavance, P. (2010), ‘Bycatch of the European purse seine
572 tuna fishery in the Atlantic Ocean for the 2003–2007 period’, *Aquatic Living Resources*
573 **23**(04), 353–362.
- 574 Blangiardo, M. and Cameletti, M. (2015), *Spatial and Spatio-temporal Bayesian Models*
575 *with R-INLA*, John Wiley & Sons.
- 576 Cameletti, M., Lindgren, F., Simpson, D. and Rue, H. (2013), ‘Spatio-temporal modeling
577 of particulate matter concentration through the SPDE approach’, *AStA Advances in*
578 *Statistical Analysis* pp. 1–23.
- 579 Cosandey-Godin, A., Teixeira Krainski, E., Worm, B. and Mills Flemming, J. (2014),
580 ‘Applying Bayesian spatio-temporal models to fisheries bycatch in the Canadian Arc-
581 tic’, *Canadian Journal of Fisheries and Aquatic Sciences* .
- 582 Davies, R., Cripps, S., Nickson, A. and Porter, G. (2009), ‘Defining and estimating global
583 marine fisheries bycatch’, *Marine Policy* **33**(4), 661–672.
- 584 Efron, B. and Tibshirani, R. J. (1994), *An introduction to the bootstrap*, CRC press.
- 585 Eriksen, E., Prozorkevich, D. and Dingsør, G. E. (2009), ‘An evaluation of 0-group abun-
586 dance indices of Barents Sea fish stocks’, *The Open Fish Science Journal* .
- 587 Fiskeridirektoratet (2005), ‘Regulations concerning fishing in the sea (in Norwegian)’.
588 **URL:** <https://lovdata.no/dokument/SF/forskrift/2004-12-22-1878>
- 589 Gelfand, A. E. (1996), ‘Model determination using sampling-based methods’, *Markov*
590 *chain Monte Carlo in practice* pp. 145–161.

591 Gelman, A., Carlin, J. B., Stern, H. S. and Rubin, D. B. (2003), *Bayesian Data Analysis*,
592 Chapman & Hall/CRC Texts in Statistical Science, 2 edn, Chapman and Hall/CRC.

593 Hopkins, C., Sargent, J. and Nilssen, E. (1993), ‘Total lipid content, and lipid and fatty
594 acid composition of the deep-water prawn *Pandalus borealis* from Balsfjord, northern
595 Norway: growth and feeding relationships’, *Marine Ecology-Progress Series* **96**, 217–
596 217.

597 ICES (1994), Report of the Arctic fisheries working group, Copenhagen, 24 August - 2
598 September 1993, Technical report.

599 Jakobsen, T. and Ozhigin, V. K. (2011), *The Barents Sea-ecosystem, resources, manage-*
600 *ment. Half a century of Russian-Norwegian cooperation*, Tapir Akademisk Forlag.

601 Jørgensen, T. (1992), ‘Long-term changes in growth of North-east Arctic cod (*Gadus*
602 *morhua*) and some environmental influences’, *ICES Journal of Marine Science: Journal*
603 *du Conseil* **49**(3), 263–278.

604 Lay, D. C. (2006), *Linear Algebra and Its Applications, Third Edition*, Person.

605 Lindgren, F., Rue, H. and Lindström, J. (2011), ‘An explicit link between Gaussian
606 fields and Gaussian Markov random fields: the stochastic partial differential equation
607 approach’, *Journal of the Royal Statistical Society: Series B (Statistical Methodology)*
608 **73**(4), 423–498.

609 Martins, T. G., Simpson, D., Lindgren, F. and Rue, H. (2013), ‘Bayesian computing with
610 INLA: new features’, *Computational Statistics & Data Analysis* **67**, 68–83.

611 Minasny, B. and McBratney, A. B. (2005), ‘The Matérn function as a general model for
612 soil variograms’, *Geoderma* **128**(3), 192–207.

613 Ottersen, G. and Loeng, H. (2000), ‘Covariability in early growth and year-class strength
614 of Barents Sea cod, haddock, and herring: the environmental link’, *ICES Journal of*
615 *Marine Science: Journal du Conseil* **57**(2), 339–348.

- 616 R Core Team (2014), *R: A Language and Environment for Statistical Computing*, R
617 Foundation for Statistical Computing, Vienna, Austria.
618 **URL:** <http://www.R-project.org>
- 619 Rue, H., Martino, S. and Chopin, N. (2009), ‘Approximate Bayesian inference for latent
620 Gaussian models by using integrated nested Laplace approximations’, *Journal of the*
621 *Royal Statistical Society: Series B (Statistical Methodology)* **71**(2), 319–392.
- 622 Seber, G. A. (1986), ‘A review of estimating animal abundance’, *Biometrics* pp. 267–292.
- 623 Spiegelhalter, D. J., Best, N. G., Carlin, B. P. and Van Der Linde, A. (2002), ‘Bayesian
624 measures of model complexity and fit’, *Journal of the Royal Statistical Society: Series*
625 *B (Statistical Methodology)* **64**(4), 583–639.
- 626 Stein, M. L. (1999), *Interpolation of spatial data: some theory for kriging*, Springer, New
627 York.
- 628 Veim, A. K., Sunnanå, K., Sandberg, P. and Gullestad, P. (1994), Bycatch of juvenile
629 fish in the shrimp fishery-management based on bioeconomic criteria, Technical Report
630 T:14, ICES.
- 631 Ye, Y. (2002), ‘Bias in estimating bycatch-to-shrimp ratios’, *Aquatic Living Resources*
632 **15**(03), 149–154.
- 633 Ye, Y., Alsaffar, A. and Mohammed, H. (2000), ‘Bycatch and discards of the Kuwait
634 shrimp fishery’, *Fisheries Research* **45**(1), 9–19.
- 635 Zuur, A. F. (2009), *Mixed effects models and extensions in ecology with R*, Springer.

Table 1: *Data used, numbers in parentheses are 90% coverage intervals.*

Data	Description
Target catch	Shrimp catch varies between 2.4 kilogram and 17.7 tons (20,3190)
Bycatch	The number of cod varies between 0 and 35775 cod (0,1008)
Time	Information about time of catch down to minutes scale
Location	Information of catch location (single point) given in longitude and latitude
Distance trawled	The distance trawled in nautical miles (2.5, 15)
Number of trawls	The number of trawls varies between one, two or three.
Circumference	The number of meshes around the opening of each trawl (1400, 3000)
Temperature	Bottom sea temperature (0.17, 9.3)
Depth	Ocean depth at catch location (227, 410)
0-group	Abundance predictions of 0-group cod per square nautical mile (0, 465408)

Table 2: *Covariates in the model*

Covariates	Type	Description
Seasonal effect	Continuous	Fourier series (3)
0-group	Continuous	Logarithm of 0-group abundance of cod
Temperature	Continuous	Bottom sea temperature
Depth	Continuous	Ocean depth at catch location
Time	Continuous	Linear covariate of time
$Z(\mathbf{s}, t)$	Continuous	Logarithm of shrimp catch per nautical mile
Area of trawl	Continuous	The square of the circumference
Number of trawls	Categorical	The number of trawls used
Night effect	Categorical	See appendix

Table 3: *Estimates and 95% credibility intervals of the significant regression coefficients.*

Covariate	Shrimp catch		Covariate	Bycatch of cod	
	Mean	95% C.I.		Mean	95% C.I.
μ	3.01	(2.49,3.51)	μ	0.52	(-0.54, 1.35)
night effect	-0.41	(-0.52,-0.31)	night effect	-0.26	(-0.40,-0.12)
area (standardized)	0.10	(0.065,0.15)	depth (standardized)	-0.17	(-0.20,-0.14)
depth (standardized)	0.085	(0.060,0.11)	double trawl	0.28	(0.16, 0.39)
double trawl	0.59	(0.51,0.67)	Z	0.24	(0.21, 0.27)
triple trawl	1.16	(0.93,1.39)	0-group	0.37	(0.17, 0.57)

Table 4: *DIC, CVD, ML and MSE values for the shrimp models and bycatch models. S, T and S-T represent spatial, yearly and spatio-temporal effects, respectively. For the spatio-temporal effect, model (5) with $q = 1$ is used, if not otherwise specified. The models with bold text correspond to the selected models.*

Random effects	DIC	CVD	ML	MSE
Shrimp model				
No random effects	21162	-38164	-38326	1.06
S	18627	-36915	-37206	0.752
S-T	14026	-35231	-36007	0.506
S and S-T	13504	-35145	-35881	0.493
S, S-T and T	13509	-35145	-35881	0.493
S and S-T with $q = 2$	14637	-35285	-35986	0.505
S and S-T with eq. (6)	15328	-35460	-36088	0.522
Bycatch model				
No random effects	55086	-27543	-27689	1.91
S	53651	-26822	-27054	1.57
S-T	48036	-24239	-25142	0.779
S and S-T	48018	-24194	-25076	0.767
S, S-T and T	47955	-24187	-25076	0.765
S, S-T with $q = 2$ and T	48320	-24277	-25165	0.785
S, S-T with eq. (6) and T	49105	-24571	-25331	0.846

Table 5: *Estimates and 95% credibility intervals of the hyperparameters.*

Shrimp catch			Bycatch of cod		
Hyperparameter	Mean	95% C.I.	Hyperparameter	Mean	95% C.I.
σ_α^2	0.97	(0.51, 1.72)	σ_α^2	1.22	(0.53, 2.48)
κ_α	0.011	(0.0071, 0.016)	κ_α	0.0064	(0.0037, 0.010)
σ_ϵ^2	0.23	(0.22, 0.25)	σ_ϵ^2	0.53	(0.50, 0.55)
σ_γ^2	0.62	(0.57, 0.68)	σ_γ^2	1.00	(0.91, 1.10)
θ_t	71 (mode)	unknown	θ_t	40 (mode)	unknown
θ_s	63 (mode)	unknown	θ_s	133 (mode)	unknown
			σ_v^2	0.20	(0.06, 0.47)

Table 6: *Predicted bycatch ratios in the Hopen area 1st. of December 2005.*

New obs.	Simple model		Aldrin et al. (2012)		Our model	
	Pred.	90%C.I.	Pred.	90%C.I.	Pred.	90%C.I.
0			1.3	(0.1, 4.7)	1.9	(0.2, 5.5)
1	7.9		1.8	(0.3, 7.1)	2.8	(0.5, 7.5)
3	21.1		4.2	(0.9, 24.8)	4.9	(1.1, 12.8)
5	16.6		3.5	(0.6, 10.1)	4.5	(1.2, 10.3)
10	7.2	(3.6, 13.5)	4.6	(1.3, 9.5)	4.5	(1.7, 9.0)
15	5.4	(2.8, 9.5)	4.2	(1.8, 6.4)	4.7	(2.0, 9.0)
21	5.6	(3.4, 8.4)	4.4	(2.2, 7.5)	4.8	(2.1, 9.1)

Table 7: Coverage of 90% and 99% prediction intervals for the shrimp catch, bycatch and bycatch ratio. The coverage is defined as the percentage of times the prediction intervals overlap with the real observations when removing and predicting every tenth trawl haul observation.

	Target	Inside P.I.	Under P.I.	Over P.I.
90%	Shrimp	90.6%	5.7%	3.7%
	Bycatch	90.6%	4.6%	4.8%
	Ratio	92.4%	3.7%	3.8%
99%	Shrimp	97.6%	1.9%	0.5%
	Bycatch	97.7%	1.1%	1.2%
	Ratio	98.4%	1.0%	0.6%

Table 8: Prior distributions

Parameter	Prior	Parameter	Prior
$\log(\sigma_\alpha^2)$	$N(0,10)$	$1/\sigma_v^2$	$\text{gamma}(1,0.00005)$
$\log(\kappa)$	$N(0,10)$	$1/\sigma_\gamma^2$	$\text{gamma}(1,0.00005)$
$1/\sigma_Z^2$	$\text{gamma}(1,0.00005)$	θ_t and θ_s	$\propto 1$
$1/\sigma_Y^2$	$\text{gamma}(1,0.00005)$	$\log(\frac{1+a}{1-a})$	$N(0, \frac{1}{0.15})$

Observations of shrimp catch in the Barents Sea

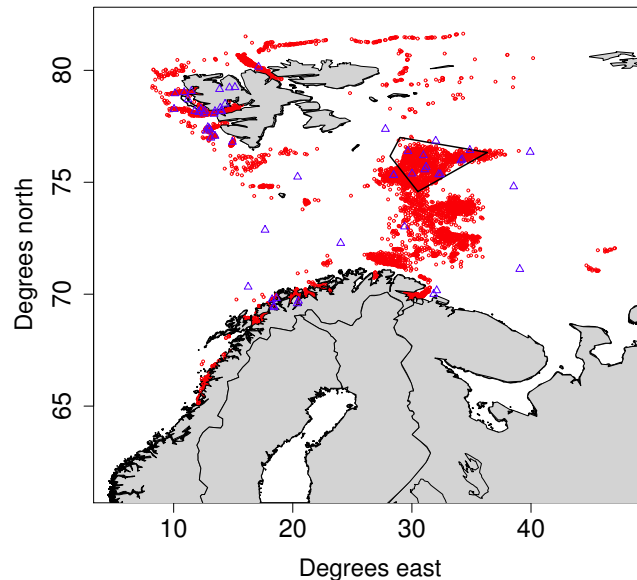


Figure 1: Map of the Barents Sea with observations of shrimp trawls represented as red dots. Blue triangles indicate observations that have been removed from the original data. The polygon described by the black lines in the middle of the Barents Sea illustrates the Hopen area where we estimate the bycatch ratio in the decision making section.

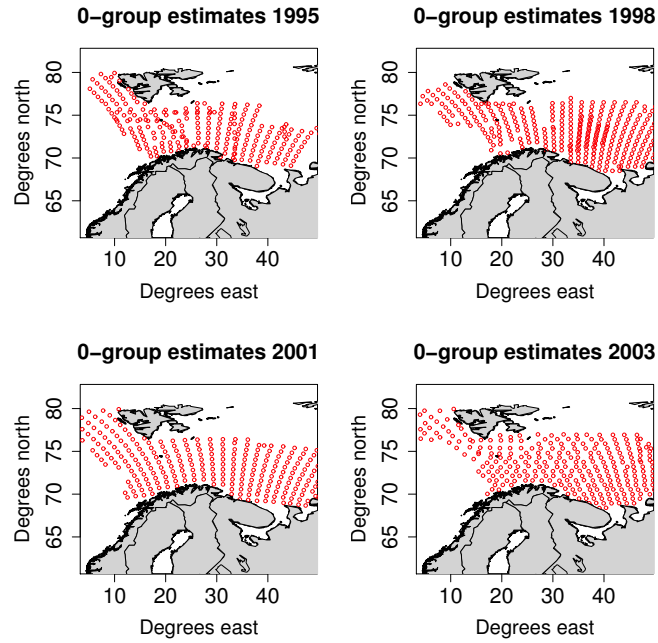


Figure 2: *Map of locations in the Barents Sea containing estimates of the 0-group of cod in four different years.*

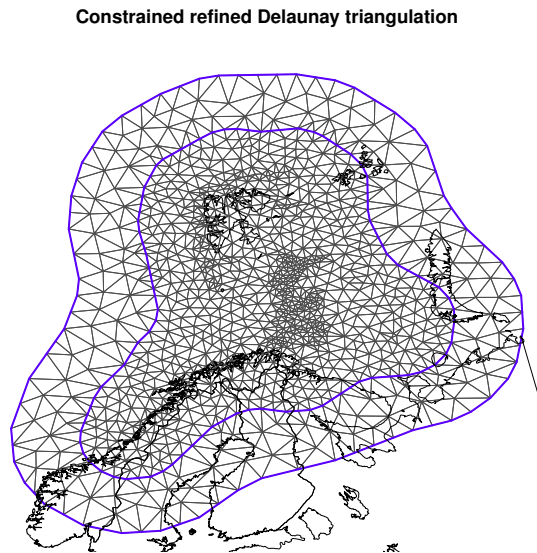


Figure 3: *The triangulation grid used for approximating the Matern covariance function of the spatial effect of shrimp catch and bycatch of juvenile cod.*

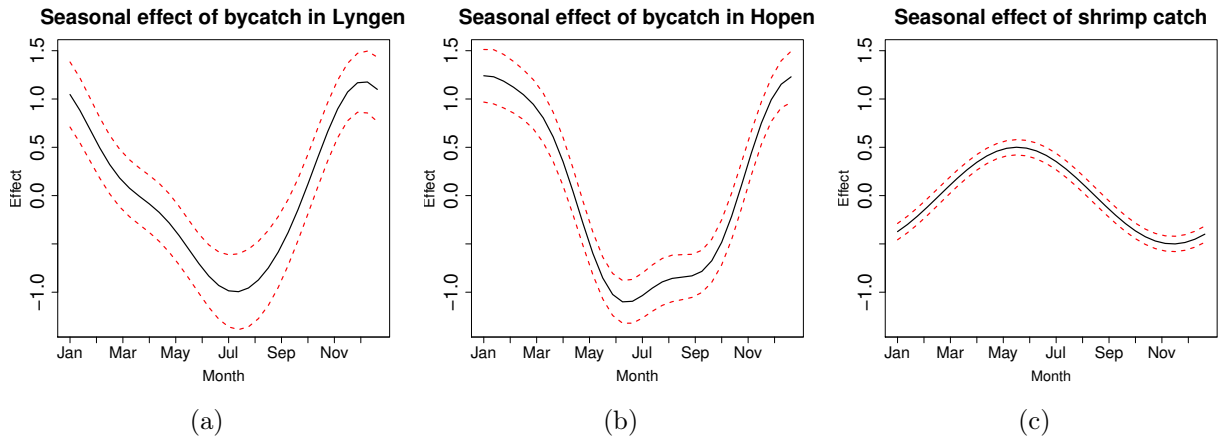


Figure 4: *The seasonal effect with 95% credibility intervals for (a) the bycatch in Lyngen (south in the area investigated), (b) the bycatch in Hopen (north in the area investigated) and (c) the shrimp catch.*

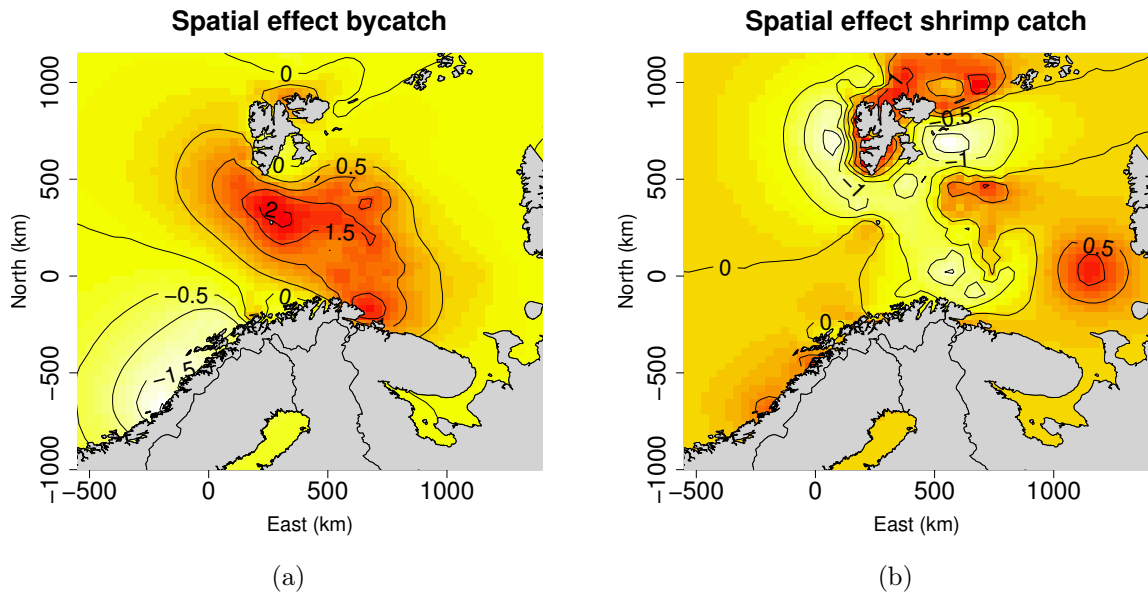


Figure 5: *The spatial effect of (a) bycatch of juvenile cod and (b) the shrimp catch. Both maps are given in UTM coordinates.*

Bycatch rate after 1st of December 2005 in Hopen

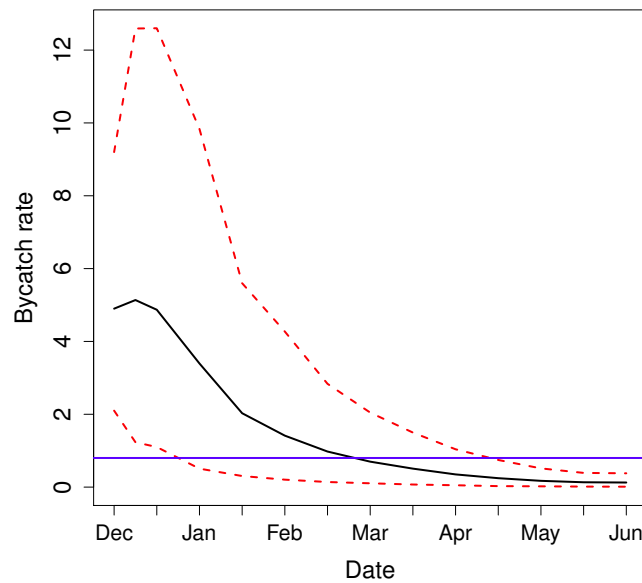


Figure 6: *Estimated bycatch ratio in the Hopen area after 1st of December 2005 based on information collected before 6th of December 2005 . The solid black line shows the mean and the dotted red lines 90% credibility intervals. The blue solid horizontal line gives the upper limit of allowed bycatch ratio.*

Bycatch rate estimates of trawl hauls in 2005 and 2006 in Hopen

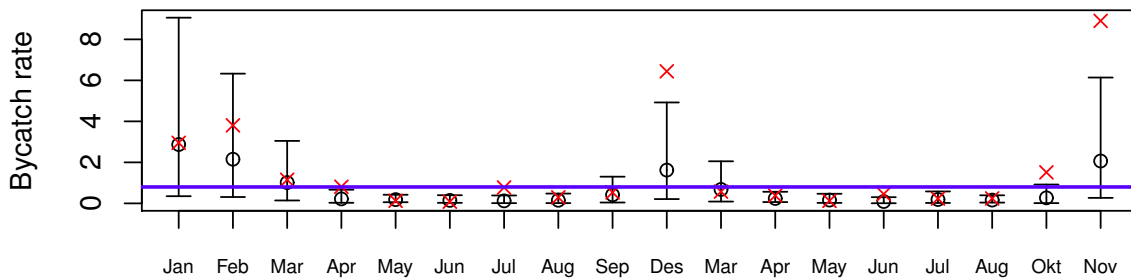


Figure 7: *Predictions with 90% prediction intervals of bycatch ratio (7) of the trawl hauls taken each month in the Hopen area in 2005 and 2006. The blue solid horizontal line shows the upper limit of allowed bycatch ratio. The red crosses are the observed bycatch ratios.*